Published in final edited form as:
J Nucl Med. 2010 March ; 51(3): 418–426. doi:10.2967/jnumed.109.071787.

Reduction of the Ring Size of Radiolabeled Lactam Bridge-Cyclized Alpha-MSH Peptide Resulting in Enhanced Melanoma Uptake

Haixun Guo[1], **Jianquan Yang**[1], **Fabio Gallazzi**[4], and **Yubin Miao**[1,2,3]

[1] College of Pharmacy, University of New Mexico, Albuquerque, NM 87131, USA

[2] Cancer Research and Treatment Center, University of New Mexico, Albuquerque, NM 87131, USA

[3] Department of Dermatology, University of New Mexico, Albuquerque, NM 87131, USA

[4] Department of Biochemistry, University of Missouri, Columbia, Missouri 65211, USA

Abstract

The purpose of this study was to examine the profound effect of the ring size of the radiolabeled lactam bridge-cyclized α-melanocyte stimulating hormone (α-MSH) peptide on its melanoma targeting properties.

Methods—A novel cyclic α-MSH peptide, DOTA-Nle-CycMSH$_{hex}$ {1,4,7,10-Tetraazacyclododecane-1,4,7,10-tetraacetic acid-Nle-c[Asp-His-DPhe-Arg-Trp-Lys]-CONH$_2$}, was synthesized and radiolabeled with ^{111}In. The melanocortin-1 (MC1) receptor binding affinity of DOTA-Nle-CycMSH$_{hex}$ was determined in B16/F1 melanoma cells. The internalization and efflux of ^{111}In-DOTA-Nle-CycMSH$_{hex}$ were examined in B16/F1 cells. The melanoma targeting properties and single photon emission computed tomography (SPECT)/CT imaging of ^{111}In-DOTA-Nle-CycMSH$_{hex}$ were determined in B16/F1 melanoma-bearing C57 mice.

Results—DOTA-Nle-CycMSH$_{hex}$ displayed 1.77 nM receptor binding affinity. ^{111}In-DOTA-Nle-CycMSH$_{hex}$ exhibited rapid internalization and extended retention in B16/F1 cells. The tumor uptake of ^{111}In-DOTA-Nle-CycMSH$_{hex}$ was 24.94 ± 4.58 and 10.53 ± 1.11% injected dose/gram (%ID/g) at 0.5 and 24 h post-injection, respectively. Greater than 82% of the injected radioactivity was cleared through the urinary system by 2 h post-injection. The tumor/kidney uptake ratios reached 2.04 and 1.70 at 2 and 4 h post-injection, respectively. Flank melanoma tumors were clearly visualized by SPECT/CT using ^{111}In-DOTA-Nle-CycMSH$_{hex}$ as an imaging probe at 2 and 24 h post-injection. The radioactivity accumulation in normal organs was low except for the kidneys at 2, 4 and 24 h post-injection.

Conclusion—The reduction of the peptide ring size dramatically increased the melanoma uptake and decreased the renal uptake of ^{111}In-DOTA-Nle-CycMSH$_{hex}$, providing a new insight into the design of novel radiolabeled lactam bridge-cyclized α-MSH peptide for melanoma imaging and treatment.

Request for reprints: Yubin Miao, 2502 Marble NE, MSC09 5360, College of Pharmacy, University of New Mexico, Albuquerque, NM 87131. Phone: (505) 925-4437; Fax: (505) 272-6749; ymiao@salud.unm.edu.
Haixun Guo, 2502 Marble NE, MSC09 5360, College of Pharmacy, University of New Mexico, Albuquerque, NM 87131. Phone: (505) 272-8034; Fax: (505) 272-6749; haguo@salud.unm.edu

Keywords

Melanoma imaging; radiolabeled cyclic peptide; alpha-melanocyte stimulating hormone; small animal imaging

Introduction

Skin cancer is the most commonly diagnosed cancer in the United States. Melanoma accounts for less than 5% of skin cancer cases but causes greater than 75% deaths of skin cancer. It is predicted that 68,720 new cases will be diagnosed and 8,650 deaths will occur in 2009 (1). Early diagnosis and prompt surgical removal are the best opportunities for a patient's cure since no curative treatment exists for metastatic melanoma. Despite the clinical use of 2-[^{18}F]fluoro-2-deoxy-D-glucose ([^{18}F]FDG) for positron emission tomography (PET) diagnosis and staging of melanoma, [^{18}F]FDG is not melanoma-specific imaging agent and is also not effective in imaging small melanoma metastases (< 5 mm) and melanomas that have primary energy sources other than glucose (2–4). Alternatively, melanocortin-1 (MC1) receptor is a distinct molecular target due to its over-expression on both human and mouse melanoma cells (5–9). Radiolabeled α-melanocyte stimulating hormone (α-MSH) peptides can bind the MC1 receptors with nanomolar binding affinities (10–20) and represent a class of promising melanoma-specific radiopharmaceuticals for melanoma imaging and therapy.

Recently, we have developed a novel class of ^{111}In-labeled lactam bridge-cyclized DOTA-conjugated α-MSH peptides for melanoma detection (21,22). Lactam bridge-cyclization was employed to improve the stabilities of the α-MSH peptides against the proteolytic degradations *in vivo* and enhance the binding affinities of the α-MSH peptides through stabilizing their secondary structures such as beta turns (23–26). The radiometal chelator DOTA was attached to the N-terminus of the lactam bridge-cyclized α-MSH peptide (12-amino acids in the peptide ring) for ^{111}In radiolabeling. For instance, ^{111}In-DOTA-GlyGlu-CycMSH (DOTA-Gly-Glu-c[Lys-Nle-Glu-His-DPhe-Arg-Trp-Gly-Arg-Pro-Val-Asp]) exhibited high MC1 receptor-mediated tumor uptake (10.40±1.40% ID/g at 2 h post-injection) in flank B16/F1 melanoma-bearing C57 mice (21). Both flank primary and pulmonary metastatic melanoma lesions were clearly visualized by small animal SPECT/CT using ^{111}In-DOTA-GlyGlu-CycMSH as an imaging probe (21,22), highlighting its potential as an effective imaging probe for melanoma detection.

One advantage of the lactam bridge-cyclized α-MSH peptide is that the peptide ring size can be finely modified by either adding or deleting amino acids without sacrificing the binding affinity of the peptide (21,22). The studies on the α-MSH peptide agonists for the MC1 receptor revealed that the lactam bridge-cyclized α-MSH peptide with a 6-amino acid peptide ring {Ac-Nle-c[Asp-His-DPhe-Arg-Trp-Lys($CONH_2$)], MT-II} displayed not only higher MC1 receptor binding affinity, but also slower MC1 receptor dissociation rate than the native α-MSH peptide {Ac-Ser-Tyr-Ser-Met-Glu-His-Phe-Arg-Trp-Gly-Lys-Pro-Val-NH_2} (27,28). Slow MC1 receptor dissociation rate might contribute to the prolonged biological activity of MT-II *in vitro* and *in vivo* (27). In this study, we conjugated the radiometal chelator DOTA to the N-terminus of the MT-II peptide to generate a novel DOTA-conjugated lactam bridge-cyclized α-MSH peptide with a 6-amino acid peptide ring (DOTA-Nle-$CycMSH_{hex}$) to examine the effect of peptide ring size on its melanoma targeting and pharmacokinetic properties. The MC1 receptor binding affinity of DOTA-Nle-$CycMSH_{hex}$ was determined in B16/F1 melanoma cells. DOTA-Nle-$CycMSH_{hex}$ was radiolabeled with ^{111}In which is a commercial available diagnostic radionuclide with a half-life of 2.8 days. The melanoma targeting and pharmacokinetic properties and SPECT/CT

imaging of ^{111}In-labeled DOTA-Nle-CycMSH$_{hex}$ were determined in B16/F1 melanoma-bearing C57 mice.

Materials and Methods

Chemicals and Reagents

Amino acid and resin were purchased from Advanced ChemTech Inc. (Louisville, KY) and Novabiochem (San Diego, CA). DOTA-tri-t-butyl ester was purchased from Macrocyclics Inc. (Richardson, TX). $^{111}InCl_3$ was purchased from Trace Life Sciences, Inc. (Dallas, TX). ^{125}I-Tyr^2-[Nle^4, D-Phe^7]-α-MSH {^{125}I-(Tyr^2)-NDP-MSH} was obtained from PerkinElmer, Inc. (Waltham, MA). All other chemicals used in this study were purchased from Thermo Fischer Scientific (Waltham, MA) and used without further purification. B16/F1 melanoma cells were obtained from American Type Culture Collection (Manassas, VA).

Peptide Synthesis

DOTA-Nle-CycMSH$_{hex}$ was synthesized using standard fluorenylmethyloxycarbonyl (Fmoc) chemistry. Briefly, intermediate scaffold of (tBu)$_3$DOTA-Nle-Asp(O-2-PhiPr)-His(Trt)-DPhe-Arg(Pbf)-Trp(Boc)-Lys(Dde) was synthesized on H_2N-Sieber amide resin by an Advanced ChemTech multiple-peptide synthesizer (Louisville, KY). The protecting group of Dde was removed by 2% hydrazine for peptide cyclization. The protecting group of 2-phenylisopropyl from the Asp residue was removed and the protected peptide was cleaved from the resin treating with a mixture of 2.5% of trifluoroacetic acid (TFA) and 5% of triisopropylsilane for 1 h. After the precipitation with ice-cold ether and characterization by liquid chromatography-mass spectroscopy (LC-MS), the protected peptide was dissolved in H_2O/CH_3CN (30:70) and lyophilized to remove the reagents such as TFA and triisopropylsilane. The protected peptide was further cyclized by coupling the carboxylic group from the Asp with the epsilon amino group from the Lys. The cyclization reaction was achieved by an overnight reaction in dimethylformamide (DMF) using benzotriazole-1-yl-oxy-tris-pyrrolidino-phosphonium-hexafluorophosphate (PyBOP) as a coupling agent in the presence of N,N-diisopropylethylamine (DIEA). After the characterization by LC-MS, the cyclized protected peptide was dissolved in H_2O/CH_3CN (30:70) and lyophilized to remove the reagents such as PyBOP and DIEA. The protecting groups were totally removed by treating with a mixture of TFA, thioanisole, phenol, water, ethanedithiol and triisopropylsilane (87.5:2.5:2.5:2.5:2.5:2.5) for 4 h at room temperature (25 °C). The peptide was precipitated and washed with ice-cold ether four times, purified by reverse phase-high performance liquid chromatography (RP-HPLC) and characterized by LC-MS.

In vitro Competitive Binding Assay

The IC_{50} value of DOTA-Nle-CycMSH$_{hex}$ was determined by *in vitro* competitive binding assay according to our previously published procedure (21). B16/F1 cells were harvested and seeded into a 24-well cell culture plate (5×10^5 cells/well) and incubated at 37°C overnight. After being washed twice with binding medium {Dulbecco's Modified Eagle's Medium with 25 mM *N*-(2-hydroxyethyl)-piperazine-*N*′-(2-ethanesulfonic acid), pH 7.4, 0.2% bovine serum albumin (BSA), 0.3 mM 1,10-phenathroline}, the cells were incubated at room temperature (25°C) for 2 h with approximately 60,000 cpm of ^{125}I-Tyr^{2-}NDP-MSH in the presence of increasing concentrations (10^{-12} to 10^{-5} M) of DOTA-Nle-CycMSH$_{hex}$ in 0.3 mL of binding medium. The reaction medium was aspirated after the incubation. The cells were rinsed twice with 0.5 mL of ice-cold pH 7.4, 0.2% BSA/0.01 M phosphate buffered saline (PBS) and lysed in 0.5 mL of 1 N NaOH for 5 minutes. The activities associated with cells were measured in a Wallac 1480 automated gamma counter (PerkinElmer, NJ). The IC_{50} value of the peptide was calculated using Prism software (GraphPad Software, La Jolla, CA).

Peptide Radiolabeling with ^{111}In

^{111}In-DOTA-Nle-CycMSH$_{hex}$ was prepared in a 0.5 M NH_4OAc-buffered solution at pH 4.5 according to our published procedure (21). Briefly, 50 μL of $^{111}InCl_3$ {37–74 MBq (1–2 mCi) in 0.05 M HCl aqueous solution}, 10 μL of 1 mg/mL DOTA-Nle-CycMSH$_{hex}$ aqueous solution and 400 μL of 0.5 M NH_4OAc (pH 4.5) were added into a reaction vial and incubated at 75°C for 45 min. After the incubation, 10 μL of 0.5% EDTA aqueous solution was added into the reaction vial to scavenge potential unbound $^{111}In^{3+}$ ions. The radiolabeled peptide was purified to single species by Waters RP-HPLC (Milford, MA) on a Grace Vydac C-18 reverse phase analytical column (Deerfield, IL) using a 20-min gradient of 18–28% acetonitrile in 20 mM HCl aqueous solution with a flow rate of 1.0 mL/min. Purified peptide sample was purged with N_2 gas for 20 minutes to remove the acetonitrile. The pH of final solution was adjusted to 7.4 with 0.1 N NaOH and sterile normal saline for animal studies. *In vitro* serum stability of HPLC-purified ^{111}In-DOTA-Nle-CycMSH$_{hex}$ was determined by incubation in mouse serum at 37°C for 24 h and monitored for degradation by RP-HPLC.

Cellular Internalization and Efflux of ^{111}In-DOTA-Nle-CycMSH$_{hex}$

Cellular internalization and efflux of ^{111}In-DOTA-Nle-CycMSH$_{hex}$ were evaluated in B16/F1 melanoma cells. After being washed twice with the binding medium, the B16/F1 cells seeded in cell culture plates were incubated at 25°C for 20, 40, 60, 90 and 120 min (n=3) in the presence of approximate 200,000 counts per minute (cpm) of HPLC-purified ^{111}In-DOTA-Nle-CycMSH$_{hex}$. After incubation, the reaction medium was aspirated and the cells were rinsed with 2×0.5 mL of ice-cold pH 7.4, 0.2% BSA/0.01 M PBS. Cellular internalization of ^{111}In-DOTA-Nle-CycMSH$_{hex}$ was assessed by washing the cells with acidic buffer [40 mM sodium acetate (pH 4.5) containing 0.9% NaCl and 0.2% BSA] to remove the membrane-bound radioactivity. The remaining internalized radioactivity was obtained by lysing the cells with 0.5 mL of 1 N NaOH for 5 min. Membrane-bound and internalized ^{111}In activities were counted in a gamma counter. Cellular efflux of ^{111}In-DOTA-Nle-CycMSH$_{hex}$ was determined by incubating the B16/F1 cells with ^{111}In-DOTA-Nle-CycMSH$_{hex}$ for 2 h at 25°C, removing non-specific-bound activity with 2×0.5 mL of ice-cold PBS rinse, and monitoring radioactivity released into cell culture medium. At time points of 20, 40, 60, 90 and 120 min, the radioactivities on the cell surface and inside the cells were separately collected and counted in a gamma counter.

Biodistribution Studies

All the animal studies were conducted in compliance with Institutional Animal Care and Use Committee approval. The mice were housed five animals per cage in sterile micro-isolator cages in a temperature- and humidity-controlled room with a 12-h light/12-h dark schedule. The pharmacokinetics of ^{111}In-DOTA-Nle-CycMSH$_{hex}$ was determined in B16/F1 melanoma-bearing C57 female mice (Harlan, Indianapolis, IN). C57 mice were subcutaneously inoculated on the right flank with 1×10^6 B16/F1 cells. The weight of tumors reached approximately 0.2 g 10 days post cell inoculation. Each melanoma-bearing mouse was injected with 0.037 MBq (1 μCi) of ^{111}In-DOTA-Nle-CycMSH$_{hex}$ via the tail vein. Groups of 5 mice were sacrificed at 0.5, 2, 4 and 24 h post-injection, and tumors and organs of interest were harvested, weighed and counted. Blood values were taken as 6.5% of the whole-body weight. The tumor uptake specificity of ^{111}In-DOTA-Nle-CycMSH$_{hex}$ was determined by co-injecting 10 μg of unlabeled [Nle^4, D-Phe^7]- α-MSH (NDP-MSH), a linear α-MSH peptide analogue with picomolar affinity for the MC1 receptor present on the melanoma cells. To examine whether *L*-lysine co-injection can reduce the renal uptake or not, a group of 5 mice were injected with a mixture of 12 mg of *L*-lysine and 0.037 MBq (1 μCi) of ^{111}In-DOTA-Nle-CycMSH$_{hex}$. The mice were sacrificed at 2 h post-injection. The tumor and organs of interest were harvested, weighed and counted.

Melanoma Imaging with ^{111}In-DOTA-Nle-CycMSH$_{hex}$

Two B16/F1 melanoma-bearing C57 mice (10 days post the cell inoculation) were injected with 37 MBq (1 mCi) of ^{111}In-DOTA-Nle-CycMSH$_{hex}$ via the tail vein, respectively. The mice were sacrificed for small animal SPECT/CT (Nano-SPECT/CT®, Bioscan) imaging at 2 and 24 h post-injection. The 9-min CT imaging was immediately followed by the whole-body SPECT imaging. The SPECT scans of 24 projections were acquired and total acquisition time was approximately 60 min. Reconstructed data from SPECT and CT were visualized and co-registered using InVivoScope (Bioscan, Washington DC).

Urinary Metabolites of ^{111}In-DOTA-Nle-CycMSH$_{hex}$

The mouse used for the imaging study (2 h post-injection) described above was euthanized and the urine was collected for indentifying the metabolites. The urinary sample was centrifuged at 16,000g for 5 min prior to the HPLC analysis. The radioactive metabolite in the urine was analyzed by injecting aliquots of urine into the HPLC. A 20-min gradient of 18–28% acetonitrile/20 mM HCl was used for the urine analysis.

Statistical Analysis

Statistical analysis was performed using the Student's t-test for unpaired data. A 95% confidence level was chosen to determine the significance between the tumor uptakes of ^{111}In-DOTA-Nle-CycMSH$_{hex}$ with or without NDP-MSH co-injection, and between the renal uptakes of ^{111}In-DOTA-Nle-CycMSH$_{hex}$ with or without *L*-lysine co-injection in the biodistribution studies described above. Differences at the 95% confidence level ($p<0.05$) were considered significant.

Results

To examine the profound effect of the peptide ring size on the melanoma and kidney uptakes of the ^{111}In-labeled lactam bridge-cyclized α-MSH peptide, a novel peptide of DOTA-Nle-CycMSH$_{hex}$ was synthesized and purified by RP-HPLC. The identity of the peptide was confirmed by electrospray ionization mass spectrometry (EIMS MW: 1368.5; Calculated MW: 1368.2). DOTA-Nle-CycMSH$_{hex}$ displayed greater than 95% purity with 30% overall synthetic yield. The schematic structures of DOTA-Nle-CycMSH$_{hex}$ and DOTA-GlyGlu-CycMSH are shown in Figure 1. Figure 2 illustrates the synthetic scheme of DOTA-Nle-CycMSH$_{hex}$. The competitive binding curve of DOTA-Nle-CycMSH$_{hex}$ is presented in Figure 3A. The IC_{50} value of DOTA-Nle-CycMSH$_{hex}$ was 1.77 nM in B16/F1 cells.

The peptide was readily labeled with ^{111}In in 0.5 M ammonium acetate at pH 4.5 with greater than 95% radiolabeling yield. ^{111}In-DOTA-Nle-CycMSH$_{hex}$ was completely separated from its excess non-labeled peptide by RP-HPLC. The retention time of ^{111}In-DOTA-Nle-CycMSH$_{hex}$ was 10.7 min. ^{111}In-DOTA-Nle-CycMSH$_{hex}$ showed greater than 98% radiochemical purity after the HPLC purification. ^{111}In-DOTA-Nle-CycMSH$_{hex}$ was stable in mouse serum at 37 °C for 24 h. Only the ^{111}In-DOTA-Nle-CycMSH$_{hex}$ was detected by RP-HPLC after 24 h of incubation.

Cellular internalization and efflux of ^{111}In-DOTA-Nle-CycMSH$_{hex}$ were evaluated in B16/F1 cells. Figures 3B and 3C illustrate the cellular internalization and efflux of ^{111}In-DOTA-Nle-CycMSH$_{hex}$, respectively. ^{111}In-DOTA-Nle-CycMSH$_{hex}$ exhibited rapid cellular internalization and extended cellular retention. There were 72.9±3.5% and 88.3±0.7% of the cellular uptake of ^{111}In-DOTA-Nle-CycMSH$_{hex}$ activity internalized in the B16/F1 cells at 20 and 120 min post incubation, respectively. Cellular efflux results demonstrated that 89.5±1.9% of internalized ^{111}In-DOTA-Nle-CycMSH$_{hex}$ activity remained inside the cells 2 h after incubating cells in culture medium.

The melanoma targeting and pharmacokinetic properties of ^{111}In-DOTA-Nle-CycMSH$_{hex}$ were determined in B16/F1 melanoma-bearing C57 mice. The biodistribution results of ^{111}In-DOTA-Nle-CycMSH$_{hex}$ are shown in Table 1. ^{111}In-DOTA-Nle-CycMSH$_{hex}$ exhibited very rapid high melanoma uptake and prolonged tumor retention in melanoma-bearing mice. At 0.5 h post-injection, ^{111}In-DOTA-Nle-CycMSH$_{hex}$ reached its peak tumor uptake value of 24.94 ± 4.58% ID/g. There were 17.01 ± 2.54% ID/g and 10.53 ± 1.11% ID/g of the ^{111}In-DOTA-Nle-CycMSH$_{hex}$ activity remained in the tumors at 4 and 24 h post-injection, respectively. In melanoma uptake blocking study, the tumor uptake of ^{111}In-DOTA-Nle-CycMSH$_{hex}$ with 10 μg of non-radiolabeled NDP-MSH co-injection was only 4.2% of the tumor uptake without NDP-MSH co-injection at 2 h after dose administration ($p<0.05$), demonstrating that the tumor uptake was specific and MC1 receptor-mediated. Whole-body clearance of ^{111}In-DOTA-Nle-CycMSH$_{hex}$ was rapid, with approximately 82% of the injected radioactivity cleared through the urinary system by 2 h post-injection (Table 1). Normal organ uptakes of ^{111}In-DOTA-Nle-CycMSH$_{hex}$ were low (<1.89% ID/g) except for the kidneys at 2, 4 and 24 h post-injection. High tumor/blood and high tumor/normal organ uptake ratios were achieved as early as 0.5 h post-injection (Table 1). As the major excretion pathway of ^{111}In-DOTA-Nle-CycMSH$_{hex}$, the kidney uptake value was 16.20 ± 4.32% ID/g at 0.5 h post-injection and decreased to 9.31± 0.91% ID/g at 24 h post-injection. The tumor to kidney uptake ratios of ^{111}In-DOTA-Nle-CycMSH$_{hex}$ are presented in Figure 4. The tumor/kidney uptake ratios of ^{111}In-DOTA-Nle-CycMSH$_{hex}$ were 2.04, 1.70 and 1.13 at 2, 4 and 24 h post-injection. Co-injection of NDP-MSH didn't reduce the renal uptake of the ^{111}In-DOTA-Nle-CycMSH$_{hex}$ activity at 2 h post-injection, indicating that the renal uptake was not MC1 receptor-mediated. Co-injection of *L*-lysine significantly ($p<0.05$) reduced the kidney uptake value by 30% at 2 h post-injection (Table 1).

Two B16/F1 melanoma-bearing C57 mice were separately injected with 37 MBq (1 mCi) of ^{111}In-DOTA-Nle-CycMSH$_{hex}$ through the tail vein to visualize the tumors at 2 and 24 h post dose administration. The whole-body SPECT/CT images are presented in Figures 5A and 5B. Flank melanoma tumors were clearly visualized by SPECT/CT at 2 and 24 h post-injection of ^{111}In-DOTA-Nle-CycMSH$_{hex}$. Both images showed high tumor to normal organ uptake ratios except for the kidneys, which was coincident with the biodistribution results. Urinary metabolite of ^{111}In-DOTA-Nle-CycMSH$_{hex}$ was analyzed by RP-HPLC 2 h post-injection. Figure 5C illustrates the urinary HPLC profile of ^{111}In-DOTA-Nle-CycMSH$_{hex}$. ^{111}In-DOTA-Nle-CycMSH$_{hex}$ remained intact in the urine 2 h post-injection.

Discussion

Cyclization strategies using disulfide bridge, lactam bridge and metal coordination have been successfully employed to cyclize the α-MSH peptides to enhance the binding affinities and *in vivo* stabilities of the peptides (23–26). Both ^{111}In-labeled metal-cyclized and lactam bridge-cyclized α-MSH peptides exhibited greater melanoma uptake and lower renal uptake values than those of ^{111}In-labeled disulfide bridge-cyclized α-MSH peptide (21,29). We have reported a novel class of melanoma-specific ^{111}In-labeled lactam bridge-cyclized α-MSH peptides for both primary and metastatic melanoma imaging (21,22). ^{111}In-DOTA-GlyGlu-CycMSH (Fig. 1), with a 12-amino acid peptide ring, exhibited great potential as a melanoma-specific imaging probe in detecting both primary and metastatic melanoma lesions (21,22). However, the tumor uptake value of ^{111}In-DOTA-GlyGlu-CycMSH was 60.15% of the tumor uptake value of ^{111}In-DOTA-Re(Arg^{11})CCMSH, whereas the kidney uptake value of ^{111}In-DOTA-GlyGlu-CycMSH was 1.5 times the renal uptake value of ^{111}In-DOTA-Re(Arg^{11})CCMSH at 2 h post-injection in B16/F1 melanoma-bearing C57 mice (17,21). The structural differences between ^{111}In-DOTA-GlyGlu-CycMSH and ^{111}In-DOTA-Re(Arg^{11})CCMSH (Fig. 1) indicated that smaller size of the peptide ring might contribute to the more favorable melanoma targeting and pharmacokinetic properties

of ^{111}In-DOTA-Re(Arg^{11})CCMSH since there was a 8-amino acid peptide ring in ^{111}In-DOTA-Re(Arg^{11})CCMSH whereas there was a 12-amino acid peptide ring in ^{111}In-DOTA-GlyGlu-CycMSH. Moreover, It was reported that the lactam bridge-cyclized α-MSH peptide with a 6-amino acid peptide ring {Ac-Nle-c[Asp-His-DPhe-Arg-Trp-Lys($CONH_2$)]} displayed not only higher MC1 receptor binding affinity, but also slower MC1 receptor dissociation rate than the native α-MSH peptide (27). Therefore, we synthesized a novel DOTA-conjugated lactam bridge-cyclized peptide with a 6-amino acid peptide ring {DOTA-Nle-CycMSH$_{hex}$} to examine the profound effect of the peptide ring size on the tumor and kidney uptakes in this study.

The conjugation of DOTA to the N-terminus of the peptide and the reduction of the peptide ring size did not sacrifice the MC1 receptor binding affinity of DOTA-Nle-CycMSH$_{hex}$. DOTA-Nle-CycMSH$_{hex}$ exhibited 1.77 nM MC1 receptor binding affinity in B16/F1 melanoma cells (Fig. 3A), whereas DOTA-GlyGlu-CycMSH and DOTA-Re(Arg^{11})CCMSH displayed 0.90 and 2.10 nM MC1 receptor binding affinities in B16/F1 cells (17,21). ^{111}In-DOTA-Nle-CycMSH$_{hex}$ displayed rapid internalization and prolonged retention in B16/F1 melanoma cells, highlighting its potential as an effective imaging probe for melanoma detection, as well as its potential as a therapeutic agent for melanoma treatment when labeled with a therapeutic radionuclide. As we anticipated, the strategy of reducing the ring size of the lactam bridge-cyclized α-MSH peptide resulted in improved tumor uptake and prolonged tumor retention. Compared to ^{111}In-DOTA-GlyGlu-CycMSH with a 12-amino acid peptide ring, ^{111}In-DOTA-Nle-CycMSH$_{hex}$ (Fig. 1) only had a 6-amino acid peptide ring. The tumor uptake value (19.39 ± 2.72% ID/g) of ^{111}In-DOTA-Nle-CycMSH$_{hex}$ was 1.86 times the tumor uptake value of ^{111}In-DOTA-GlyGlu-CycMSH 2 h post-injection in B16/F1 melanoma-bearing C57 mice. ^{111}In-DOTA-Nle-CycMSH$_{hex}$ also exhibited prolonged tumor retention than ^{111}In-DOTA-GlyGlu-CycMSH. At 24 h post-injection, 54.3% of ^{111}In-DOTA-Nle-CycMSH$_{hex}$ activity at 2 h post-injection (10.53 ± 1.11% ID/g) remained in the tumors (Table 1), whereas only 22.8% of the ^{111}In-DOTA-GlyGlu-CycMSH radioactivity at 2 h post-injection (2.37 ± 0.28% ID/g) remained inside the tumors. Urinary analysis demonstrated that the ^{111}In-DOTA-Nle-CycMSH$_{hex}$ remained intact 2 h post-injection (Fig. 5C). It is likely that both high *in vivo* stability of ^{111}In-DOTA-Nle-CycMSH$_{hex}$ and low MC1 receptor dissociation rate (15) contributed to the rapid high melanoma uptake (24.94 ± 4.58% ID/g at 0.5 h post-injection) and prolonged tumor retention (10.53 ± 1.11% ID/g at 24 h post-injection) of ^{111}In-DOTA-Nle-CycMSH$_{hex}$ in B16/F1 melanoma-bearing C57 mice.

The reduction of the peptide ring size also decreased the non-specific kidney uptake of ^{111}In-DOTA-Nle-CycMSH$_{hex}$ compared to ^{111}In-DOTA-GlyGlu-CycMSH (21) at 2 and 4 h post-injection. The renal uptake values of ^{111}In-DOTA-Nle-CycMSH$_{hex}$ were only 72.8% and 82.4% of the renal uptake values of ^{111}In-DOTA-GlyGlu-CycMSH at 2 and 4 h post-injection, respectively. The renal uptake value of ^{111}In-DOTA-Nle-CycMSH$_{hex}$ was further reduced with *L*-lysine co-injection by 30% at 2 h post-injection, demonstrating that the electrostatic interaction between ^{111}In-DOTA-Nle-CycMSH$_{hex}$ and the kidney cells played an important role in the renal uptake of ^{111}In-DOTA-Nle-CycMSH$_{hex}$. The synergistic effects of an increase of the tumor uptake and a decrease of the renal uptake dramatically improved the tumor to kidney uptake ratios of ^{111}In-DOTA-Nle-CycMSH$_{hex}$ at all time points investigated in this study. Improved tumor uptake and decreased kidney uptake resulted in superior tumor/kidney uptake ratios of ^{111}In-DOTA-Nle-CycMSH$_{hex}$ than those of ^{111}In-DOTA-CycMSH-CycMSH at 2, 4 and 24 h post-injection. The tumor to kidney uptake ratios of ^{111}In-DOTA-Nle-CycMSH$_{hex}$ were 2.55, 2.79 and 4.35 times the tumor to kidney uptake ratios of ^{111}In-DOTA-GlyGlu-CycMSH at 2, 4 and 24 h post-injection, respectively (Fig. 4). ^{111}In-DOTA-Nle-CycMSH$_{hex}$ remained intact in the urine 2 (Fig. 5C) whereas all of ^{111}In-DOTA-GlyGlu-CycMSH transformed into two polar

metabolites in the urine 2 h post-injection (19), which might contribute to the decreased renal uptake of ^{111}In-DOTA-Nle-CycMSH$_{hex}$.

Recently, ^{99m}Tc-labeled lactam bridge-cyclized α-MSH peptides {[Ac-Nle^4,Asp^5,D-Phe^7,Lys^{11}(pz-^{99m}Tc(CO)$_3$)]α-MSH$_{4–11}$ and ^{99m}Tc(CO)$_3$-pz-βAla-Nle-cyclo[Asp-His-D-Phe-Arg-Trp-Lys]-NH$_2$} have been reported for melanoma targeting (30,31). ^{99m}Tc(CO)$_3$-pz-βAla-Nle-cyclo[Asp-His-D-Phe-Arg-Trp-Lys]-NH$_2$ exhibited superior melanoma uptake (11.31 ± 1.81 %ID/g) to [Ac-Nle^4,Asp^5,D-Phe^7,Lys^{11}(pz-^{99m}Tc(CO)$_3$)]α-MSH$_{4–11}$ (4.24 ± 0.94 %ID/g) at 4 h post-injection in B16/F1 melanoma-bearing C57 mice. However, ^{99m}Tc(CO)$_3$-pz-βAla-Nle-cyclo[Asp-His-D-Phe-Arg-Trp-Lys]-NH$_2$ displayed high accumulation and prolonged retention in both liver (22.86 ± 1.17 %ID/g) and kidneys (32.12 ± 1.57 %ID/g) at 4 h post-injection, which might limit its potential application in metastatic melanoma imaging. In this study, the tumor uptake of ^{111}In-DOTA-Nle-CycMSH$_{hex}$ was 1.5 times the tumor uptake of ^{99m}Tc(CO)$_3$-pz-βAla-Nle-cyclo[Asp-His-D-Phe-Arg-Trp-Lys]-NH$_2$ at 4 h post-injection, whereas the liver and renal uptake values of ^{111}In-DOTA-Nle-CycMSH$_{hex}$ were only 7.5% and 31.1% of the ^{99m}Tc(CO)$_3$-pz-βAla-Nle-cyclo[Asp-His-D-Phe-Arg-Trp-Lys]-NH$_2$ at 4 h post-injection. Dramatic increase of the tumor uptake and decrease of the liver and kidney uptakes of ^{111}In-DOTA-Nle-CycMSH$_{hex}$ were likely due to the structural differences between ^{99m}Tc(CO)$_3$-pz-βAla-Nle-cyclo[Asp-His-D-Phe-Arg-Trp-Lys]-NH$_2$ and ^{111}In-DOTA-Nle-CycMSH$_{hex}$.

Currently, metal-cyclized ^{111}In-DOTA-Re(Arg^{11})CCMSH showed the highest melanoma uptake among all reported ^{111}In-labeled linear and cyclic α-MSH peptides (17). The tumor uptake values of ^{111}In-DOTA-Re(Arg^{11})CCMSH were 17.29 ± 2.49, 17.41 ± 5.63 and 8.19 ± 1.63 % ID/g at 2, 4 and 24 h post-injection, respectively (17). Remarkably, ^{111}In-DOTA-Nle-CycMSH$_{hex}$ exhibited 1.12, 0.98 and 1.29 times the tumor uptake values of ^{111}In-DOTA-Re(Arg^{11})CCMSH at 2, 4 and 24 h post-injection, respectively. Meanwhile, ^{111}In-DOTA-Nle-CycMSH$_{hex}$ showed slightly higher but similar renal uptake values to ^{111}In-DOTA-Re(Arg^{11})CCMSH at 2 and 4 h post-injection. ^{111}In-DOTA-Nle-CycMSH$_{hex}$ exhibited comparable tumor to kidney ratios as ^{111}In-DOTA-Re(Arg^{11})CCMSH at 2 and 24 h post-injection despite that the tumor to kidney uptake ratio of ^{111}In-DOTA-Nle-CycMSH$_{hex}$ was 28% less than that of ^{111}In-DOTA-Re(Arg^{11})CCMSH at 4 h post-injection. It was reported that a single-dose treatment of 7.4 MBq of ^{212}Pb-labeled DOTA-Re(Arg^{11})CCMSH (200 μCi) resulted in 44% cures in B16/F1 melanoma-bearing mice (11). Accordingly, it would be likely that the treatment of ^{212}Pb-labeled DOTA-Nle-CycMSH$_{hex}$ would yield similar quantitative therapeutic effect for melanoma in the future since ^{111}In-DOTA-Nle-CycMSH$_{hex}$ displayed comparable tumor to kidney ratios as ^{111}In-DOTA-Re(Arg^{11})CCMSH at 2 and 24 h post-injection.

Conclusion

The ring size of the ^{111}In-labeled lactam bridge-cyclized α-MSH peptide exhibited a profound effect on its melanoma targeting and pharmacokinetic properties. The reduction of the peptide ring size dramatically increased the melanoma uptake and decreased the renal uptake of ^{111}In-DOTA-Nle-CycMSH$_{hex}$, providing a new insight into the design of novel radiolabeled lactam bridge-cyclized α-MSH peptide for melanoma imaging and treatment.

Acknowledgments

We thank Mr. Benjamin M. Gershman for his technical assistance. This work was supported in part by the Southwest Melanoma SPORE Developmental Research Program, the DOD grant W81XWH-09-1-0105 and the NIH grant NM-INBRE P20RR016480. The image in this article was generated by the Keck-UNM Small Animal Imaging Resource established with funding from the W.M. Keck Foundation and the University of New Mexico Cancer Research and Treatment Center (NIH P30 CA118100).

Financial Support: This work was supported in part by the Southwest Melanoma SPORE Developmental Research Program, the DOD grant W81XWH-09-1-0105 and the NIH grant NM-INBRE P20RR016480. The image in this article was generated by the Keck-UNM Small Animal Imaging Resource established with funding from the W.M. Keck Foundation and the University of New Mexico Cancer Research and Treatment Center (NIH P30 CA118100).

References

1. Jemal A, Siegel R, Ward E, Hao Y, Xu J, Thun MJ. Cancer statistics, 2009. CA Cancer J Clin 2009;59:225–249. [PubMed: 19474385]
2. Alonso O, Martinez M, Delgado L, et al. Staging of regional lymph nodes in melanoma patients by means of ^{99m}Tc-MIBI scintigraphy. J Nucl Med 2003;44:1561–1565. [PubMed: 14530467]
3. Nabi HA, Zubeldia JM. Clinical application of ^{18}F-FDG in oncology. J Nucl Med Technol 2002;30:3–9. [PubMed: 11948260]
4. Dimitrakopoulou-Strauss A, Strauss LG, Burger C. Quantitative PET studies in pretreated melanoma patients: A comparison of 6-[^{18}F]fluoro-L-DOPA with ^{18}F-FDG and ^{15}O-water using compartment and non-compartment analysis. J Nucl Med 2001;42:248–256. [PubMed: 11216523]
5. Miao Y, Whitener D, Feng W, Owen NK, Chen J, Quinn TP. Evaluation of the human melanoma targeting properties of radiolabeled alpha-melanocyte stimulating hormone peptide analogues. Bioconjug Chem 2003;14:1177–1184. [PubMed: 14624632]
6. Miao Y, Owen NK, Whitener D, Gallazzi F, Hoffman TJ, Quinn TP. In vivo evaluation of ^{188}Re-labeled alpha-melanocyte stimulating hormone peptide analogs for melanoma therapy. Int J Cancer 2002;101:480–487. [PubMed: 12216078]
7. Chen J, Cheng Z, Hoffman TJ, Jurisson SS, Quinn TP. Melanoma-targeting properties of ^{99m}technetium-labeled cyclic alpha-melanocyte-stimulating hormone peptide analogues. Cancer Res 2000;60:5649–5658. [PubMed: 11059756]
8. Siegrist W, Solca F, Stutz S, et al. Characterization of receptors for alpha-melanocyte-stimulating hormone on human melanoma cells. Cancer Res 1989;49:6352–6358. [PubMed: 2804981]
9. Tatro JB, Reichlin S. Specific receptors for alpha-melanocyte-stimulating hormone are widely distributed in tissues of rodents. Endocrinology 1987;121:1900–1907. [PubMed: 2822378]
10. Miao Y, Owen NK, Fisher DR, Hoffman TJ, Quinn TP. Therapeutic efficacy of a ^{188}Re-labeled alpha-melanocyte-stimulating hormone peptide analog in murine and human melanoma-bearing mouse models. J Nucl Med 2005;46:121–129. [PubMed: 15632042]
11. Miao Y, Hylarides M, Fisher DR, et al. Melanoma therapy via peptide-targeted alpha-radiation. Clin Cancer Res 2005;11:5616–5621. [PubMed: 16061880]
12. Froidevaux S, Calame-Christe M, Tanner H, Eberle AN. Melanoma targeting with DOTA-alpha-melanocyte-stimulating hormone analogs: structural parameters affecting tumor uptake and kidney uptake. J Nucl Med 2005;46:887–895. [PubMed: 15872364]
13. Froidevaux S, Calame-Christe M, Schuhmacher J, et al. A gallium-labeled DOTA-alpha-melanocyte- stimulating hormone analog for PET imaging of melanoma metastases. J Nucl Med 2004;45:116–123. [PubMed: 14734683]
14. Froidevaux S, Calame-Christe M, Tanner H, Sumanovski L, Eberle AN. A novel DOTA-alpha-melanocyte-stimulating hormone analog for metastatic melanoma diagnosis. J Nucl Med 2002;43:1699–1706. [PubMed: 12468522]
15. Wei L, Butcher C, Miao Y, et al. Synthesis and biologic evaluation of ^{64}Cu-labeled rhenium-cyclized alpha-MSH peptide analog using a cross-bridged cyclam chelator. J Nucl Med 2007;48:64–72. [PubMed: 17204700]
16. Miao Y, Benwell K, Quinn TP. ^{99m}Tc- and ^{111}In-labeled alpha-melanocyte-stimulating hormone peptides as imaging probes for primary and pulmonary metastatic melanoma detection. J Nucl Med 2007;48:73–80. [PubMed: 17204701]
17. Cheng Z, Chen J, Miao Y, Owen NK, Quinn TP, Jurisson SS. Modification of the structure of a metallopeptide: synthesis and biological evaluation of ^{111}In-labeled DOTA-conjugated rhenium-cyclized alpha-MSH analogues. J Med Chem 2002;45:3048–3056. [PubMed: 12086490]

18. Cheng Z, Xiong Z, Subbarayan M, Chen X, Gambhir SS. ^{64}Cu-labeled alpha-melanocyte-stimulating hormone analog for MicroPET imaging of melanocortin 1 receptor expression. Bioconjug Chem 2007;18:765–772. [PubMed: 17348700]
19. Wei L, Miao Y, Gallazzi F, et al. Ga-68 labeled DOTA-rhenium cyclized α-MSH Analog for imaging of malignant melanoma. Nucl Med Biol 2007;34:945–953. [PubMed: 17998097]
20. Cantorias MV, Figueroa SD, Quinn TP, et al. Development of high-specific-activity ^{68}Ga-labeled DOTA-rhenium-cyclized alpha-MSH peptide analog to target MC1 receptors overexpressed by melanoma tumors. Nucl Med Biol 2009;36:505–13. [PubMed: 19520291]
21. Miao Y, Gallazzi F, Guo H, Quinn TP. ^{111}In-labeled lactam bridge-cyclized alpha-melanocyte stimulating hormone peptide analogues for melanoma imaging. Bioconjug Chem 2008;19:539–547. [PubMed: 18197608]
22. Guo H, Shenoy N, Gershman BM, Yang J, Sklar LA, Miao Y. Metastatic melanoma imaging with an ^{111}In-labeled lactam bridge-cyclized alpha-melanocyte-stimulating hormone peptide. Nucl Med Biol 2009;36:267–276. [PubMed: 19324272]
23. Sawyer TK, Hruby VJ, Darman PS, Hadley ME. [half-Cys^{4},half-Cys^{10}]-α-melanocyte-stimulating hormone: a cyclic α-melanotropin exhibiting superagonist biological activity. Proc Natl Acad Sci USA 1982;79:1751–1755. [PubMed: 6281785]
24. Al-Obeidi F, Hadley ME, Pettitt BM, Hruby VJ. Design of a new class of superpotent cyclic α-melanotropins based on quenched dynamic simulations. J Am Chem Soc 1989;111:3413–3416.
25. Al-Obeidi F, de L Castrucci AM, Hadley ME, Hruby VJ. Potent and prolonged-acting cyclic lactam analogs of α-melanotropin: design based on molecular dynamics. J Med Chem 1989;32:2555–2561. [PubMed: 2555512]
26. Fung S, Hruby VJ. Design of cyclic and other templates for potent and selective peptide α-MSH analogues. Curr Opin Chem Biol 2005;9:352–358. [PubMed: 16023401]
27. Haskell-Luevano C, Miwa H, Dickinson C, et al. Characterizations of the unusual dissociation properties of melanotropin peptides from the melanocortin receptor, hMC1R. J Med Chem 1996;39:432–435. [PubMed: 8558511]
28. Haskell-Luevano C, Toth K, Boteju L, et al. Beta-Methylation of the Phe^{7} and Trp^{9} melanotropin side chain pharmacophores affects ligand-receptor interactions and prolonged biological activity. J Med Chem 1997;40:2740–2749. [PubMed: 9276019]
29. Chen J, Cheng Z, Owen NK, et al. Evaluation of an ^{111}In-DOTA-rhenium cyclized alpha-MSH analog: a novel cyclic-peptide analog with improved tumor-targeting properties. J Nucl Med 2001;42:1847–1855. [PubMed: 11752084]
30. Raposinho PD, Xavier C, Correia JD, Falcao S, Gomes P, Santos I. Melanoma targeting with alpha-melanocyte stimulating hormone analogs labeled with fac-[^{99m}Tc(CO)$_3$]$^{+}$: effect of cyclization on tumor-seeking properties. J Biol Inorg Chem 2008;13:449–459. [PubMed: 18183429]
31. Raposinho PD, Correia JD, Alves S, Botelho MF, Santos AC, Santos I. A ^{99m}Tc(CO)$_3$-labeled pyrazolyl–α-melanocyte-stimulating hormone analog conjugate for melanoma targeting. Nucl Med Biol 2008;35:91–99. [PubMed: 18158948]

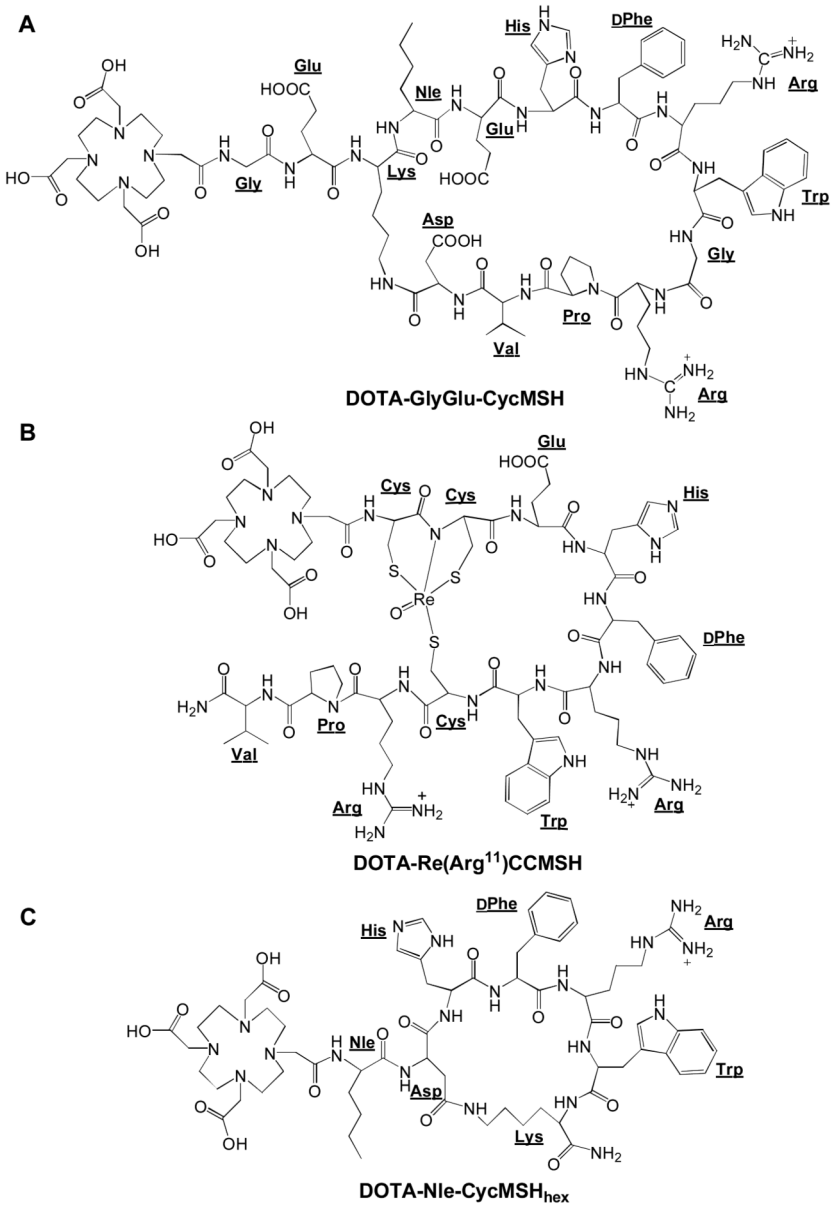

Figure 1.

Structures of DOTA-GlyGlu-CycMSH (A), DOTA-Re(Arg^{11})CCMSH (B) and DOTA-Nle-CycMSH$_{hex}$ (C).

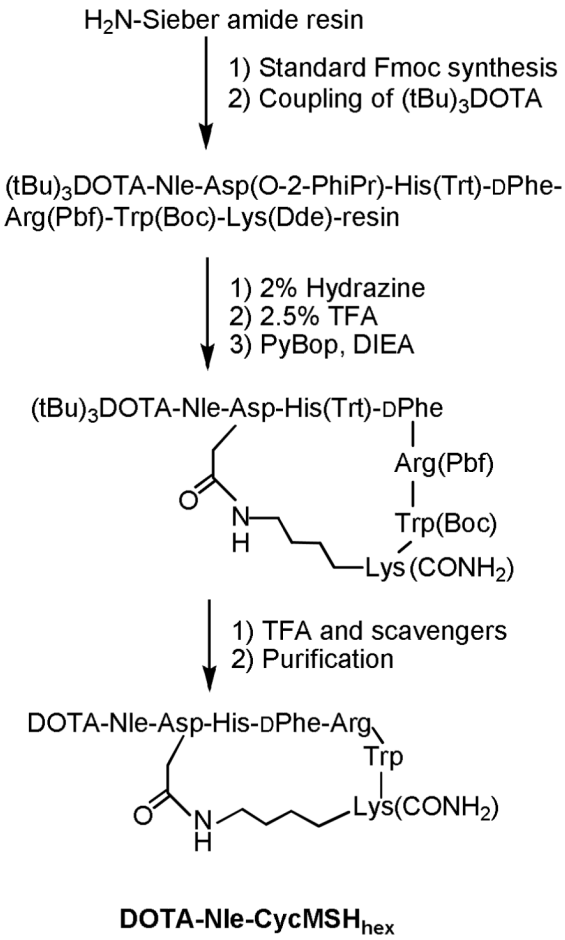

Figure 2.
Synthetic scheme of DOTA-Nle-CycMSH$_{hex}$.

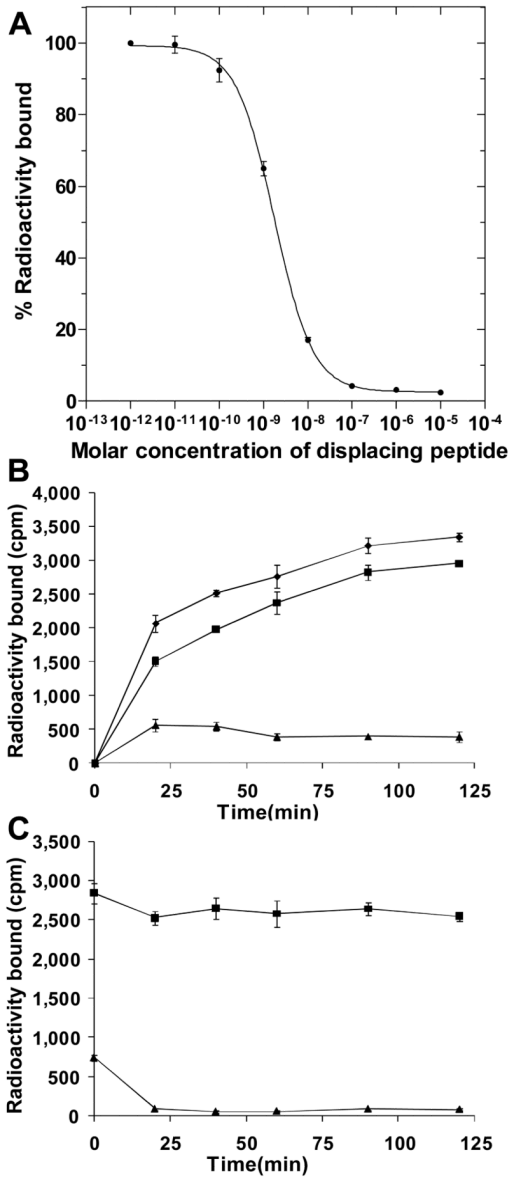

Figure 3.

The competitive binding curve (A) of DOTA-Nle-CycMSH$_{hex}$ in B16/F1 melanoma cells. The IC_{50} value of DOTA-Nle-CycMSH$_{hex}$ was 1.77 nM. Cellular internalization (B) and efflux (C) of ^{111}In-DOTA-Nle-CycMSH$_{hex}$ in B16/F1 melanoma cells at 25°C. Total bound radioactivity (◆), internalized activity (■) and cell membrane activity (▲) were presented as counts per minute (cpm).

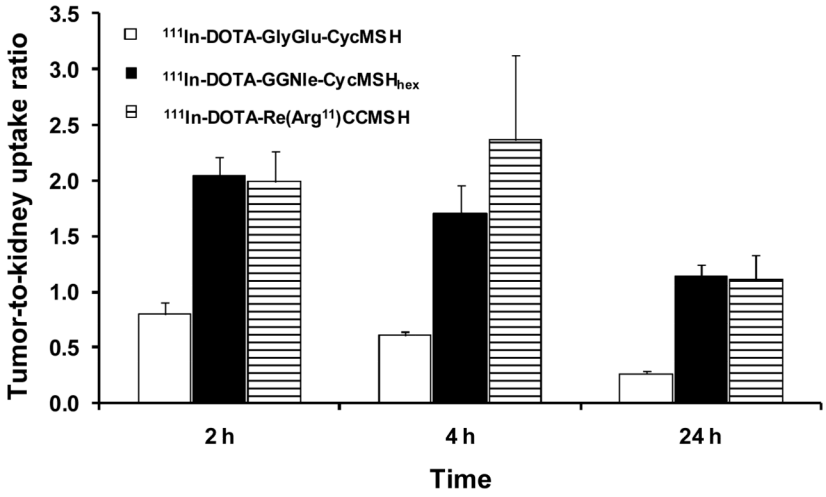

Figure 4.

Tumor to kidney uptake ratios of ^{111}In-DOTA-GlyGlu-CycMSH, ^{111}In-DOTA-Nle-CycMSH$_{hex}$ and ^{111}In-DOTA-Re(Arg^{11})CCMSH at 2, 4 and 24 h post-injection. The tumor to kidney uptake ratios of ^{111}In-DOTA-GlyGlu-CycMSH and ^{111}In-DOTA-Re(Arg^{11})CCMSH were calculated based on the results published in the references [19] and [17].

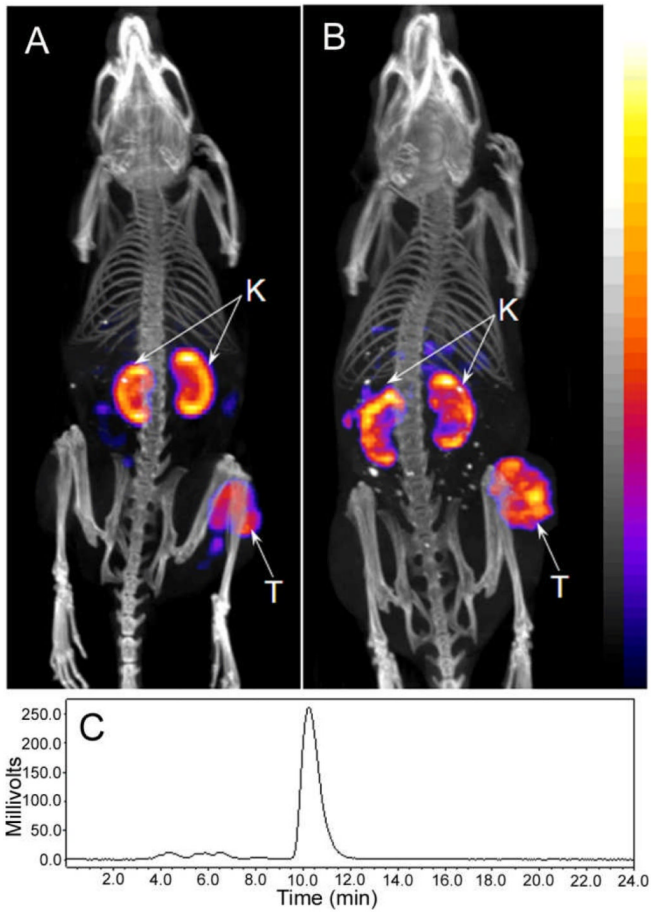

Figure 5.

Whole-body SPECT/CT images of B16/F1 flank melanoma-bearing C57 mice at 2 (A) and 24 h (B) post-injection of 37 MBq (1 mCi) of ^{111}In-DOTA-Nle-CycMSH$_{hex}$. Tumor (T) and kidneys (K) are highlighted with arrows on the images. HPLC profile (C) of radioactive urine sample of a B16/F1 melanoma-bearing C57 mouse at 2 h post-injection of ^{111}In-DOTA-Nle-CycMSH$_{hex}$. ^{111}In-DOTA-Nle-CycMSH$_{hex}$ remained intact in the urine 2 h post-injection.

Table 1

Biodistribution of ^{111}In-DOTA-Nle-CycMSH$_{hex}$ in B16/F1 melanoma-bearing C57 mice. The data were presented as percent injected dose/gram or as percent injected dose (Mean±SD, n=5)

Tissues	0.5 h	2 h	4 h	24 h	2 h NDP blockade	2 h *L*-lysine co-injection
			Percent injected dose/gram (%ID/g)			
Tumor	24.94±4.58	19.39±1.65	17.01±2.54	10.53±1.11	0.81±0.03*	14.48±3.25
Brain	0.21±0.07	0.02±0.01	0.06±0.03	0.03±0.01	0.01±0.01	0.04±0.01
Blood	3.33±0.35	0.11±0.07	0.05±0.02	0.02±0.01	0.07±0.05	0.92±0.48
Heart	1.24±0.15	0.16±0.10	0.12±0.03	0.07±0.05	0.06±0.02	0.37±0.02
Lung	2.45±0.83	0.32±0.10	0.10±0.05	0.10±0.03	0.30±0.06	0.75±0.21
Liver	2.75±0.26	1.46±0.20	1.72±0.07	1.89±0.14	1.46±0.08	1.42±0.30
Spleen	1.09±0.33	0.41±0.13	0.47±0.13	0.32±0.08	0.44±0.02	0.43±0.07
Stomach	3.20±0.98	1.25±0.24	1.49±0.12	1.34±0.42	0.36±0.14	1.64±0.78
Kidneys	16.20±4.32	9.52±0.44	9.99±1.39	9.31±0.91	11.56±0.56	6.66±0.62*
Muscle	0.60±0.22	0.15±0.08	0.10±0.08	0.03±0.01	0.02±0.01	0.10±0.08
Pancreas	1.18±0.38	0.14±0.02	0.16±0.02	0.23±0.08	0.12±0.02	0.21±0.05
Bone	1.34±0.40	0.18±0.10	0.22±0.15	0.16±0.03	0.05±0.04	0.55±0.14
Skin	4.11±0.72	0.66±0.23	0.53±0.05	0.64±0.16	0.29±0.02	1.02±0.09
			Percent injected dose (%ID)			
Intestines	2.16±0.28	1.40±0.56	3.03±1.06	1.41±0.86	1.14±0.47	1.85±0.73
Urine	57.00±3.91	82.23±5.83	84.61±5.21	87.29±3.60	92.25±1.56	76.79±5.35
			Tumor to normal tissue uptake ratio			
Tumor/Blood	7.49	176.27	340.20	526.50	11.57	15.74
Tumor/Kidneys	1.54	2.04	1.70	1.13	0.07	2.17
Tumor/Lung	10.18	60.59	170.10	105.30	2.70	19.31
Tumor/Liver	9.07	13.28	9.89	5.57	0.55	10.20
Tumor/Muscle	41.57	129.27	170.10	351.00	40.50	144.80
Tumor/Skin	6.07	29.38	32.09	16.45	2.79	14.20

*P <0.05, significance comparison between the tumor uptakes of ^{111}In-DOTA-Nle-CycMSH$_{hex}$ with or without NDP-MSH blockade, and between the kidney uptakes of ^{111}In-DOTA-Nle-CycMSH$_{hex}$ with or without *L*-lysine co-injection.